

# Lattice accommodation of epitaxial Bi(111) films on Si(001) studied with SPA-LEED and AFM

G. Jnawali, H. Hattab, B. Krenzer, and M. Horn von Hoegen\*

*Experimentelle Physik, Universität Duisburg-Essen, Lotharstr. 1, 47048 Duisburg, Germany*

(Received 19 June 2006; revised manuscript received 2 September 2006; published 29 November 2006)

The growth of Bi on a Si(001) surface is studied *in situ* by spot profile analyzing low-energy electron diffraction and *ex situ* by atomic force microscopy. A continuous epitaxial Bi(111) film with a thickness of 6 nm is grown at 150 K in a bilayer growth mode. During annealing to 450 K the lattice mismatch between Si(001) and Bi(111) is accommodated by a periodic interfacial misfit dislocation array. On this relaxed template, Bi(111) films can be grown to any desired thickness. Such films are composed of twinned and 90° rotated micrometer sized Bi(111) crystallites with a roughness of less than 0.6 nm for a 30 nm thick film.

DOI: 10.1103/PhysRevB.74.195340

PACS number(s): 68.55.Jk, 61.14.Hg, 68.35.Gy

## I. INTRODUCTION

Bismuth (Bi) is a semimetal with remarkable electronic properties which arises from its low carrier concentrations, highly anisotropic Fermi surface, and small effective carrier masses  $m^*$ .<sup>1</sup> Due to its large Fermi wavelength and long carrier mean free path  $\lambda$ , Bi has been extensively investigated for quantum transport and finite-size effects.<sup>2-4</sup> The small values of  $m^*$  and the very large value of  $\lambda$  are very advantageous in achieving large spin-relaxation lengths and are useful for the realization of spin-based electronic devices.<sup>5</sup> These unique properties also results in very large magnetoresistance effects as observed in bulk Bi<sup>6</sup> and also in Bi nanowires<sup>7,8</sup> and Bi thin films.<sup>9</sup> However, the fabrication of high-quality Bi thin films, a requirement for studying Bi's transport properties and for technological applications, as such, has been difficult. Bi thin films made by evaporation and sputtering are often polycrystalline with small grains.<sup>10,11</sup>

Bi is among the very few elements which can be grown on Si without silicide formation or intermixing at the interface. Epitaxial Bi(111) films have been successfully grown on Si(111)-(7×7).<sup>12,13</sup> Previous attempts of Bi growth on Si(001) suggested a Frank–van der Merwe mode at low temperatures ( $T < 280$  K) and a Stranski–Krastanov mode at high temperatures ( $T > 280$  K).<sup>14</sup> The deposition at low temperatures, however, is accompanied by the formation of bulk defects and increasing surface roughness.

Here we present a kinetic pathway to grow smooth and relaxed Bi(111) films on Si(001) utilizing deposition of a template film at low temperatures, followed by an annealing step at higher temperatures, and the subsequent completion to the desired film thickness. Such films are composed of both twinned and 90° rotated micrometer sized Bi(111) crystallites with a roughness of less than 0.6 nm for a 30 nm thick film. Crucial for the success is the formation of an interfacial dislocation array during the annealing step which accommodates the lattice mismatch between Bi and Si.

The film morphology, surface roughness and strain state have been studied by *in situ* spot profile analysis low-energy electron diffraction (SPA-LEED) and *ex situ* atomic force microscopy (AFM).

## II. EXPERIMENT

The experiments have been performed under ultra high vacuum conditions at a base pressure of  $2 \times 10^{-10}$  mbar.

SPA-LEED has been used either with the built-in normal incidence electron gun to characterize the surface morphology after deposition<sup>15,16</sup> or the external electron gun in a RHEED-like geometry<sup>16,17</sup> to observe diffraction spots *in vivo* during deposition. Highly oriented Si(001) samples (Wafernet, Boron doped, 8–12  $\Omega$  cm, miscut less than 0.2°) were degassed at 600 °C. The native oxide was removed by a short flash up to 1350 °C. This preparation results in a clear (2×1) LEED pattern with  $c(4 \times 2)$  stripes at room temperature. Sample cooling was carried out by a liquid nitrogen cryostat attached to the sample holder. High purity Bi (Mateck GmbH, Purity 99.9999%) was evaporated from a directly heated ceramic crucible mounted in a water-cooled copper shroud. The deposition rate of the Bi film was monitored by a quartz microbalance mounted on the evaporator. The coverage was calibrated by the observation of bilayer intensity oscillations of the (00)-spot during Bi deposition as shown in Fig. 1. The total thickness of the film was subsequently verified by *ex situ* AFM measurements.

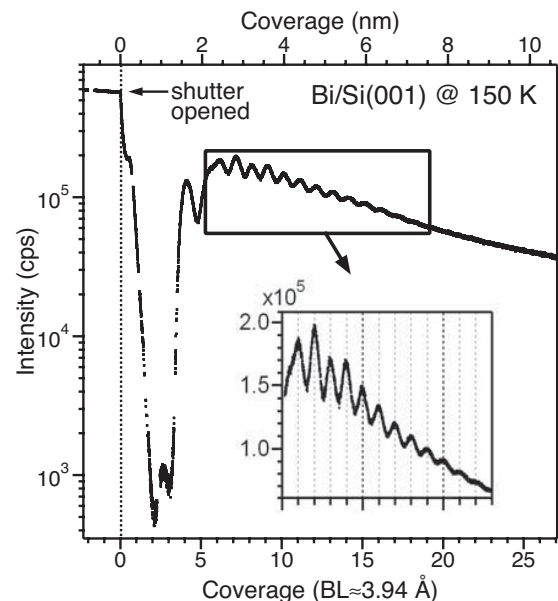


FIG. 1. Specular spot intensity vs coverage during deposition of Bi on Si(001) at 150 K. After 6 BLs, intensity oscillations with bilayer periodicity reflects Frank–van der Merwe growth mode. Damping of the oscillations is caused by kinetic roughening of the Bi film due to a barrier for interlayer diffusion.

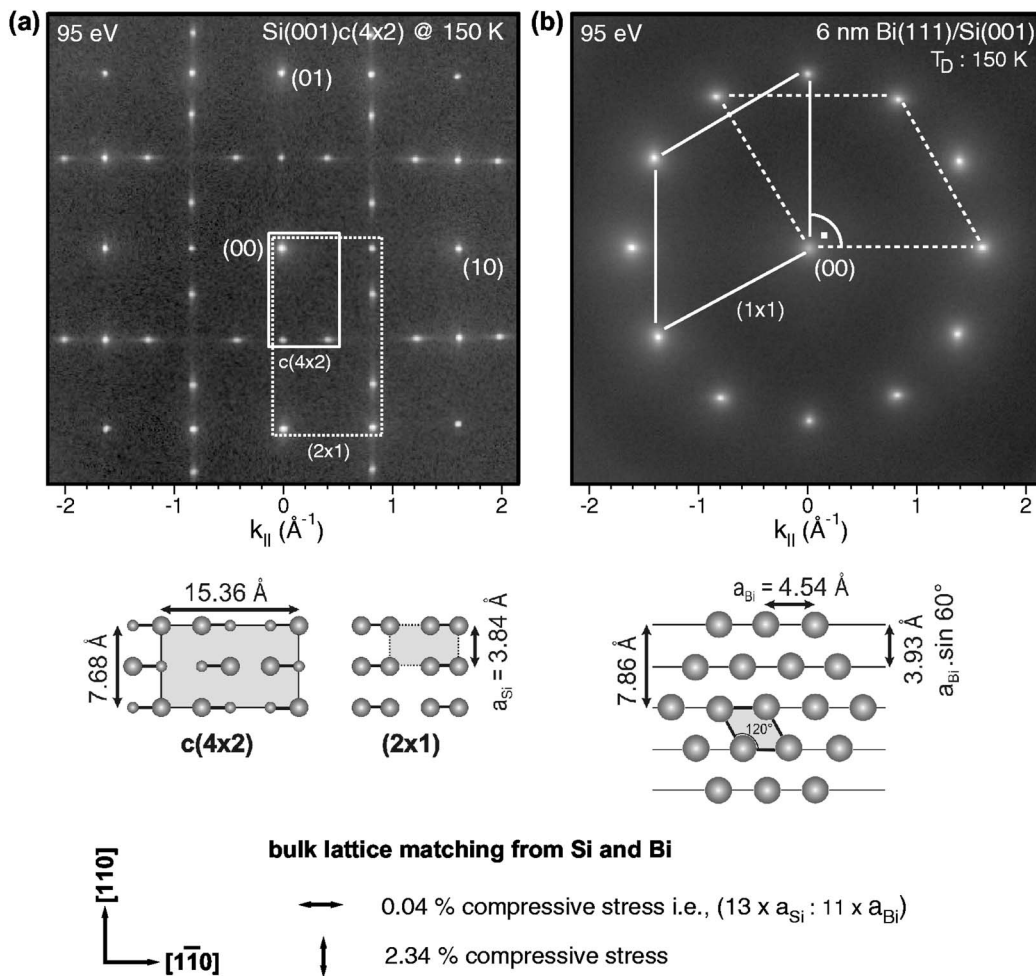


FIG. 2. (a) LEED pattern of Si(001) at 150 K. Intensity is shown in a logarithmic scale. The two reconstructions, i.e.,  $c(4 \times 2)$  and  $(2 \times 1)$ , have been indicated by the corresponding reciprocal unit cells. Top view sketches of the  $c(4 \times 2)$  and  $(2 \times 1)$  unit cells of the Si(001) surface in real space are shown below. The anti-phase dimer buckling of the  $c(4 \times 2)$  is indicated by small and large Si atoms. (b) LEED pattern of a 6 nm Bi(111) film on Si(001) after deposition at 150 K. Intensity is shown in a logarithmic scale. The quasi-12-fold symmetry is explained by the superposition of two hexagonal LEED patterns of Bi(111) rotated by  $90^\circ$ . The two corresponding reciprocal  $(1 \times 1)$  unit cells are sketched with solid and dashed lines, respectively. A sketch of the real space Bi(111) hexagonal surface lattice for one of the rotational domains is shown below. Twice the Bi(111) row separation of  $3.93 \text{ \AA}$  matches almost the separation of Si  $(2 \times 1)$  dimer rows of  $7.68 \text{ \AA}$ . The remaining lattice mismatch of 2.3% is finally adjusted by the formation of an interfacial dislocation array.

### III. RESULTS AND DISCUSSION

The fabrication of a smooth Bi film is a three step approach. In order to avoid island formation, a template is grown at a low temperature. Annealing at an elevated temperature decreases film roughness and leads to the formation of an interfacial dislocation network accommodating the lattice mismatch between Si and Bi. With further deposition at 450 K the desired Bi film thickness can be achieved.

Prior to Bi deposition the Si(001) sample was flashed to  $1300^\circ\text{C}$  for 3 s in order to desorb any adsorbates. The sample holder was kept at 150 K, which allowed a rapid cooling of the sample to 150 K. During cooling the Si(001)- $(2 \times 1)$  surface undergoes a reversible order-disorder phase transition at 200 K towards a  $c(4 \times 2)$  reconstruction.<sup>18–20</sup> The existence of sharp  $c(4 \times 2)$ -spots with a low background in the LEED pattern shown in Fig. 2(a) is a strong indication for a clean surface with low defect density.

The LEED pattern after deposition of 6 nm Bi at 150 K shows a quasi-12-fold symmetry of the first order spots with a separation of  $1.62 \text{ \AA}^{-1}$  to the central 00-spot, corresponding to a real space distance of  $3.88 \pm 0.02 \text{ \AA}$ . This pattern is explained as a superposition of two hexagonal Bi(111) domains rotated by  $90^\circ$  with respect to each other. The initial Si(001) surface consists of both  $c(4 \times 2)$  and  $c(2 \times 4)$  domains which rotates by  $90^\circ$  on neighboring terraces. The alternate buckling of the  $c(4 \times 2)$  reconstruction is destroyed by submonolayer amounts of Bi. Then the Bi(111) film obviously grows in crystallites aligned along the dimer orientation and in registry with the Si(001) surface row distance of  $3.84 \text{ \AA}$ . As a consequence, this 6 nm Bi(111) film is laterally compressed by 2.3% compared with the Bi bulk value of  $3.93 \text{ \AA}$ . The (00)-spot is slightly broadened with a full-width at half-maxima of  $0.021 \text{ \AA}^{-1}$  indicating a well-ordered continuous epitaxial Bi film with a rough surface. A similar

pattern has also been observed for the Ag(111)/Si(001) system.<sup>21</sup>

Figure 1 shows the intensity of the (00)-spot during deposition. The strong intensity drop between 1 and 3 BL (bilayer) [1 BL of Bi(111)= $1.12 \times 10^{15}$  Bi atoms/cm<sup>2</sup>] is explained by a change of film orientation as observed also for the growth of Bi(111) on Si(111).<sup>12,13</sup> Beyond the coverage of 5 BL, i.e., 2 nm, intensity oscillations with BL period indicating a Frank-van der Merwe growth mode of Bi. The bilayer growth mode with a step height of 3.93 Å has been independently confirmed by *ex situ* AFM measurements of the film which shows a step height of 4 Å at the surface. Evidence for the bilayer termination of Bi(111) has also been given by Refs. 22–24.

This 6 nm Bi film was annealed to RT by leaving the sample for 3 h without cooling and to 450 K by slowly heating the sample for 30 min. The LEED pattern shown in Fig. 3 has changed drastically: each of the twelve (10) spots is alternately elongated in the [110] or [1 $\bar{1}$ 0] direction of the Si(001) substrate. The (00)-spot is elongated cross-like in both directions. The subset of (10)-spots from one of the two Bi(111) domains, however, are elongated all in the same direction. A careful analysis exhibits a clearly resolved spot splitting of all spots into a linear series of satellite spots with increasing intensity at higher electron energies. Such phenomenon is observed when the surface undergoes a periodic height undulation with a corrugation on an angstrom scale, due to strain fields caused by an interfacial dislocation network. The periodic undulation acts as a phase grating for electrons as in optics and, therefore, all LEED spots show a splitting. From the separation of the satellite spots, which is 1.8% of the distance between integer order spots, we conclude an average distance of 210 Å between the interfacial misfit dislocations. This kind of lattice accommodation by a periodic array of interfacial dislocations has already been observed for other hetero systems such as Ge on Si(111)<sup>25</sup> or Ag on Si(001).<sup>21</sup>

The driving force for the formation of this dislocation array is the strain in the Bi film due to the lattice mismatch between Bi(111) and Si(001). Surprisingly, both lattices could be matched commensurably without a buildup of a

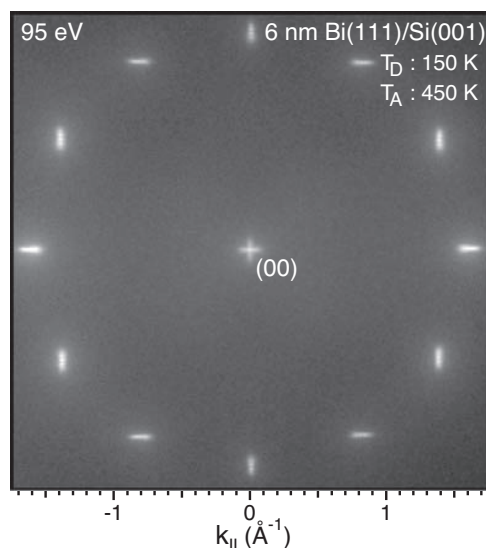


FIG. 3. LEED pattern of a 6 nm Bi(111) film on Si(001) after deposition at 150 K and annealing to 450 K. The splitting of each spot into a series of satellites due to a periodic surface undulation originating from an interfacial misfit dislocation array is clearly visible. Intensity is shown in a logarithmic scale.

large amount of strain: in the [110] direction the atomic row distance of 3.93 Å of the bulk Bi(111) interface plane almost fits well with the Si dimer distance of 3.84 Å. The remaining mismatch of only 2.3% (the compressive stress in the Bi film) is almost accommodated by the formation of the dislocation array. In the perpendicular [1 $\bar{1}$ 0] direction both lattices are commensurate with a ratio of  $13 \times 3.84$  Å (Si dimer distance) to  $11 \times 4.54$  Å (the atomic distance of the Bi(111) crystal along the [1 $\bar{1}$ 0]-directions) (see Fig. 2).

Although this 6 nm Bi(111) film was already relaxed, smooth, and continuous, we continued with the deposition of additional Bi in order to minimize the periodic surface height undulation. With increasing thickness the strain fields at the surface overlap more and more and gradually disappear for film thicknesses exceeding the distance between the dislocations.<sup>25</sup>

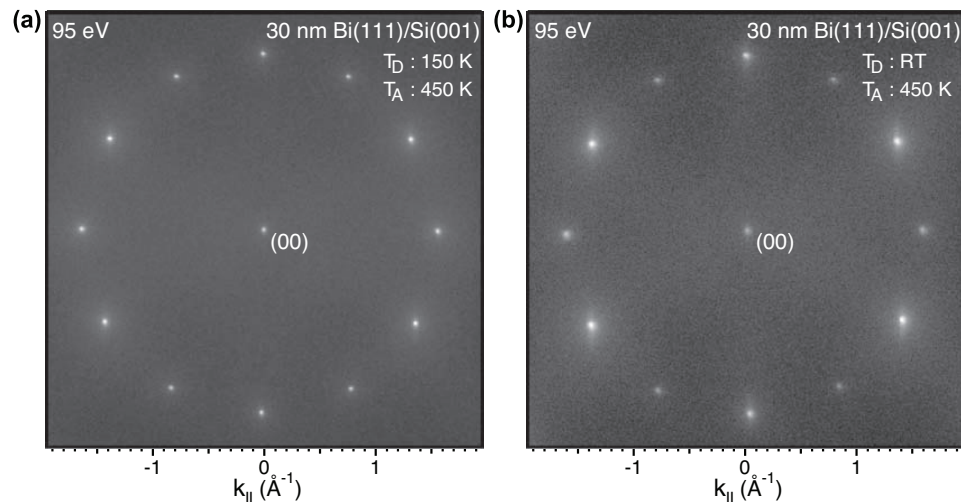


FIG. 4. (a) LEED pattern of a 30 nm Bi(111) film on Si(001) prepared according to the recipe described in this paper. (b) LEED pattern of 30 nm Bi(111) film on Si(001) deposited at RT and annealed to 450 K.



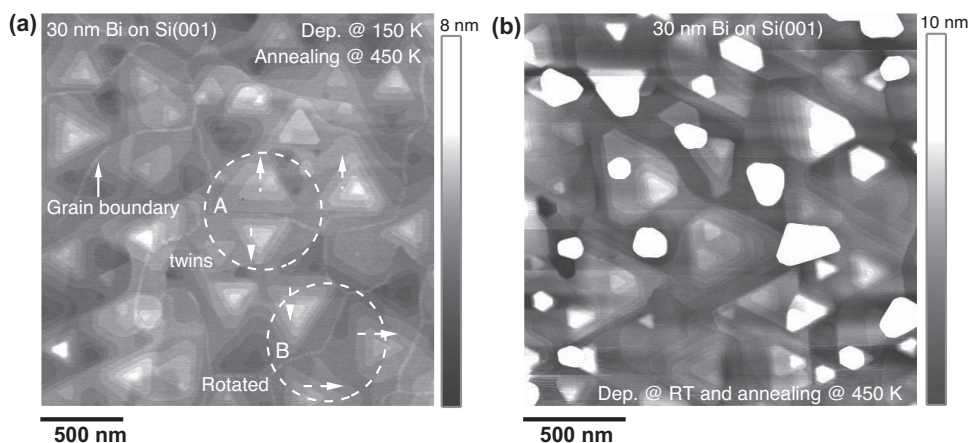


FIG. 5. (a) AFM image ( $2.5 \times 2.5 \mu\text{m}^2$ ) of a 30 nm Bi(111) film on Si(001) prepared according to the recipe described in this paper. Arrows show the azimuthal orientation of neighbored Bi crystallites separated by grain boundaries. Dashed circles A and B highlight twins and  $90^\circ$  rotated triangular Bi islands, respectively. (b) AFM image ( $2 \times 2 \mu\text{m}^2$ ) of 30 nm Bi film deposited at RT and annealed to 450 K. The overall surface roughness has increased by a factor of 5 and clusters (white areas) with a height up to 9 nm are present.

The LEED pattern after an additional deposition of 24 nm of Bi on top of the 6 nm template film at 450 K is shown in Fig. 4(a). The width of the (00)-spot has decreased to  $0.012 \text{ \AA}^{-1}$  reflecting the absence of surface roughness and small angle mosaics in the film. From the absence of spot splitting it is obvious that the periodic strain fields have cancelled each other out.

From the separation of  $1.595 \text{ \AA}^{-1}$  of the first order spots to the central (00)-spot we derived a row distance of  $3.93 \text{ \AA}$ , corresponding to an atomic distance of  $4.55 \pm 0.02 \text{ \AA}$  in the (111) surface plane which matches almost perfectly the bulk value of  $4.54 \text{ \AA}$ . The Bi film is relaxed and shows the bulk lattice parameters.

Finally, we compare the film morphology of this film with another 30 nm Bi-film which was prepared by deposition of Bi at RT and subsequent annealing to 450 K. The LEED pattern of the latter is shown in Fig. 4(b) and exhibits broader spots and a higher background indicating a rough surface.

The difference in both recipes becomes clearly visible in *ex situ* noncontact atomic force microscopy (NC-AFM) images shown in Fig. 5. Figure 5(a) shows a film grown according to the above described fashion: growth of 6 nm film at 150 K, anneal to 450 K and additional deposition of 24 nm Bi at 450 K. The surface shows large triangular islands with bilayer step heights of  $4 \text{ \AA}$ . The typical terrace width is always larger than 100 nm. The overall root mean square (RMS) roughness is calculated to be  $\Delta = 0.6 \text{ nm}$ . In contrast to this the film grown at RT and annealed to 450 K [as shown in Fig. 5(b)] has islands of almost the same size and shape but the surface is much rougher, with a RMS value of  $\Delta = 7.8 \text{ nm}$ . Beside an increased overall roughness the existence of clusters with a height up to 9 nm [the white areas in Fig. 5(b)] deteriorate the film quality.

In both images the two Bi(111) crystallites rotated by  $90^\circ$  with a micrometer size are present and can be identified by the  $90^\circ$  rotation of the orientation of the triangular islands [the dashed circle B in Fig. 5(a)]. In addition, twinned areas can also be identified by a  $180^\circ$  rotation of the triangular islands [the dashed circle A in Fig. 5(a)]. Twinning of the Bi(111) crystallites occurs because there is no left-right orientational preference with respect to the Si dimer rows. The grain boundaries between those crystallites (both the twinned and the rotated ones) can easily be identified and are indicated by arrows in Fig. 5(a).

#### IV. SUMMARY

We presented a kinetic pathway for the growth of continuous, epitaxial, and relaxed Bi(111) films on Si(001): the growth of a 6 nm template film at lower temperatures hinders island formation and annealing at higher temperatures enables the formation of an interfacial misfit dislocation array which accommodates the lattice mismatch. A further deposition at elevated temperature allows the growth to the desired thickness. Due to the twofold symmetry of the underlying Si(001) substrate both twinned and  $90^\circ$ -rotated Bi(111) crystallites with micrometer size are formed. Nevertheless, the films are perfectly flat on a 100 nm scale and show a rms roughness of only 0.6 nm on a length scale of  $2.5 \mu\text{m}$ .

#### ACKNOWLEDGMENTS

We wish to thank F. J. Meyer zu Heringdorf for the AFM measurements. Financial support from the Deutsche Forschungsgemeinschaft through SFB 616 “Energy Dissipation at Surfaces” is gratefully acknowledged.

\*Corresponding author. Email address: horn-von-hoegen@uni-due.de

- <sup>1</sup>G. E. Smith, G. A. Baraff, and J. M. Rowell, *Phys. Rev.* **135**, A1118 (1964).
- <sup>2</sup>Yu. F. Komnik, E. I. Bukhshtab, Yu. V. Nikitin, and V. V. Andrievskii, *Zh. Eksp. Teor. Fiz.* **60**, 669 (1971) [*Sov. Phys. JETP* **33**, 364 (1971)].
- <sup>3</sup>N. Garcia, Y. H. Kao, and M. Strongin, *Phys. Rev. B* **5**, 2029 (1972).
- <sup>4</sup>M. Lu, R. J. Zieve, A. van Hulst, H. M. Jaeger, T. F. Rosenbaum, and S. Radelaar, *Phys. Rev. B* **53**, 1609 (1996).
- <sup>5</sup>K. I. Lee, M. H. Jeun, J. Y. Chang, S. H. Han, J. G. Ha, and W. Y. Lee, *Phys. Status Solidi B* **241**, 1510 (2004).
- <sup>6</sup>J. H. Mangez, J. P. Issi, and J. Heremans, *Phys. Rev. B* **14**, 4381 (1976).
- <sup>7</sup>K. Liu, C. L. Chien, P. C. Searson, and K. Yu-Zhang, *Appl. Phys. Lett.* **73**, 1436 (1998).
- <sup>8</sup>Z. Zhang, X. Sun, M. S. Dresselhaus, J. Y. Ying, and J. P. Heremans, *Appl. Phys. Lett.* **73**, 1589 (1998).
- <sup>9</sup>F. Y. Yang, K. Liu, K. Hong, D. H. Reich, P. C. Searson, and C. L. Chien, *Science* **284**, 1335 (1999).
- <sup>10</sup>D. E. Beutler and N. Giordano, *Phys. Rev. B* **38**, 8 (1988).
- <sup>11</sup>J. Chang, H. Kim, J. Han, M. H. Jeon, and W. Y. Lee, *J. Appl. Phys.* **98**, 023906 (2005).
- <sup>12</sup>T. Nagao, J. T. Sadowski, M. Saito, S. Yaginuma, Y. Fujikawa, T. Kogure, T. Ohno, Y. Hasegawa, S. Hasegawa, and T. Sakurai, *Phys. Rev. Lett.* **93**, 105501 (2004).
- <sup>13</sup>M. Kammler and M. Horn-von Hoegen, *Surf. Sci.* **576**, 56 (2005).
- <sup>14</sup>W. C. Fan, A. Ignatiev, and N. J. Wu, *Surf. Sci.* **235**, 169 (1990).
- <sup>15</sup>U. Scheithauer, G. Meyer, and M. Henzler, *Surf. Sci.* **178**, 441 (1986).
- <sup>16</sup>M. Horn-von Hoegen, *Z. Kristallogr.* **214**, 18 (1999).
- <sup>17</sup>M. Horn von Hoegen, J. Falta, and M. Henzler, *Thin Solid Films* **183**, 213 (1989).
- <sup>18</sup>D. J. Chadi, *Phys. Rev. Lett.* **43**, 43 (1979); T. Tabata, T. Aruga, and Y. Murata, *Surf. Sci.* **179**, L63 (1987).
- <sup>19</sup>R. A. Wolkow, *Phys. Rev. Lett.* **68**, 2636 (1992).
- <sup>20</sup>K. Inoue, Y. Morikawa, K. Terakura, and M. Nakayama, *Phys. Rev. B* **49**, 14774 (1994).
- <sup>21</sup>M. Horn-von Hoegen, T. Schmidt, G. Meyer, D. Winau, and K. H. Rieder, *Phys. Rev. B* **52**, 10764 (1995).
- <sup>22</sup>V. S. Edelman, D. Y. Sharvin, I. N. Khlyustikov, and A. M. Troyanovskii, *Europhys. Lett.* **34**, 115 (1996).
- <sup>23</sup>H. Mönig, J. Sun, Yu. M. Koroteev, G. Bihlmayer, J. Wells, E. V. Chulkov, K. Pohl, and Ph. Hofmann, *Phys. Rev. B* **72**, 085410 (2005).
- <sup>24</sup>Ph. Hofmann, *Surf. Sci.* **81**, 191 (2006).
- <sup>25</sup>M. Horn-von Hoegen, A. Al-Falou, H. Pietsch, B. H. Müller and M. Henzler, *Surf. Sci.* **298**, 29 (1993).